CO Oxidation Catalyzed by Oxide-Supported $Au_{25}(SR)_{18}$ Nanoclusters and Identification of Perimeter Sites as Active Centers

Xiaotao Nie,[†,§] Huifeng Qian,[‡] Qingjie Ge,[†,*] Hengyong Xu,[†] and Rongchao Jin[‡,*]

[†]Dalian National Laboratory for Clean Energy, Dalian Institute of Chemical Physics, Chinese Academy of Sciences, Dalian 116023, China, [‡]Department of Chemistry, Carnegie Mellon University, Pittsburgh, Pennsylvania 15213, United States, and [§]Graduate University of Chinese Academy of Sciences, Beijing 100049, China

ABSTRACT In this work, we explore the catalytic application of atomically monodisperse, thiolate-protected $Au_{25}(SR)_{18}$ (where R = CH_2CH_2Ph) nanoclusters supported on oxides for CO oxidation. The solution phase nanoclusters were directly deposited onto various oxide supports (including TiO_2, CeO_2, and Fe_2O_3), and the as-prepared catalysts were evaluated for the CO oxidation reaction in a fixed bed reactor. The supports exhibited a strong effect, and the $Au_{25}(SR)_{18}/CeO_2$ catalyst was found to be much more active than the others. Interestingly, O_2 pretreatment of the catalyst at 150 °C for 1.5 h significantly enhanced the catalytic activity. Since this pretreatment temperature is well below the thiolate desorption temperature (~200 °C), the thiolate ligands should remain on the Au_{25} cluster surface, indicating that the CO oxidation reaction is catalyzed by intact $Au_{25}(SR)_{18}/CeO_2$. We further found that increasing the O_2 pretreatment temperature to 250 °C (above the thiolate desorption temperature) did not lead to any further increase in activity at all reaction temperatures from room temperature to 100 °C. These results are in striking contrast with the common thought that surface thiolates must be removed—as is often done in the literature work—before the catalyst can exert high catalytic activity. The 150 °C O_2-pretreated $Au_{25}(SR)_{18}/CeO_2$ catalyst offers ~94% CO conversion at 80 °C and ~100% conversion at 100 °C. The effect of water vapor on the catalytic performance is also investigated. Our results imply that the perimeter sites of the interface of $Au_{25}(SR)_{18}/CeO_2$ should be the active centers. The intact structure of the $Au_{25}(SR)_{18}$ catalyst in the CO oxidation process allows one to gain mechanistic insight into the catalytic reaction.

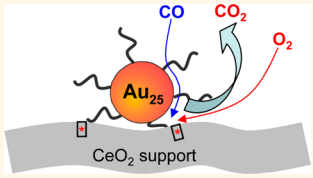

KEYWORDS: $Au_{25}(SR)_{18}$ nanocluster · supported catalyst · CO oxidation · water vapor · pretreatment temperature

Carbon monoxide oxidation catalyzed by Au nanoparticles on oxide supports has been extensively investigated since the seminal work by Haruta *et al.* two decades ago.[1−6] The significant feature of nanogold catalysts lies in their extraordinarily high activity for CO oxidation at mild or even low temperatures (*e.g.*, −70 °C). The CO oxidation process is of importance in practical processes, such as the removal of CO impurity from H_2 in fuel cells.[7] With respect to the fundamental mechanism of nanogold-catalyzed CO oxidation, despite the tremendous work, the catalytic mechanism is still under debate.[5,6] Gold catalysts prepared by conventional methods such as impregnation of $HAuCl_4$ are apparently not well-defined, manifested in the presence of residual gold ions, or few-atom clusters, as well as a broad size distribution of nanoparticles on the support. Such catalysts pose major challenges for basic science studies, especially in revealing (1) the real species that catalyzes CO oxidation (metallic nanogold or gold ions), (2) the authentic catalytic active sites (*e.g.*, gold surface or the gold/support interface), (3) the nature of the support for the catalyst (*e.g.*, the drastic effect of certain supports), and (4) the effect of water vapor, just to name a few.

To understand the reaction mechanism of gold-catalyzed CO oxidation, well-defined gold catalysts are apparently of critical importance. Toward this goal, a promising approach is to first prepare well-defined nanoparticles in solution phase, followed by deposition of solution phase well-defined nanoparticles onto the support. This strategy ensures uniform gold nanoparticles on the support, although such uniformity may be affected if high-temperature calcination is executed. To prepare uniform gold nanoparticles, there have been many methods available in the literature owing to the rapid development of nanoscience in recent years. We are particularly interested in ultrasmall gold nanoparticles, which are often called nanoclusters due to their non-metallic nature.[8] A successful size-focusing methodology has been developed for preparing a number of atomically

* Address correspondence to geqj@dicp.ac.cn, rongchao@andrew.cmu.edu.

Received for review March 7, 2012 and accepted June 3, 2012.

Published online June 12, 2012
10.1021/nn301019f

precise gold nanoclusters protected by thiolate ligands (referred to as $Au_n(SR)_m$, where n and m denote the number of gold atoms and thiolate ligands, respectively).[8,9] The $Au_n(SR)_m$ nanoclusters, such as $Au_{25}(SR)_{18}$, $Au_{38}(SR)_{24}$, $Au_{144}(SR)_{60}$, *etc.*, are particularly robust as they result from size-focusing under harsh conditions.[8−13] During the harsh size-focusing process, those unstable sizes in the crude product (with a properly controlled size distribution) were crashed or converted, leaving behind the most stable size.[8,9] This strategy has permitted precise control of $Au_n(SR)_m$ nanoclusters at the atomic level, and nanoclusters of molecular purity have been attained. In some cases, correlation of the structure of gold nanoclusters with electronic, optical, magnetic, and catalytic properties has been achieved.[14−23] Herein, our interest is to explore the catalytic properties of the new class of $Au_n(SR)_m$ nanomaterial. The well-defined nature of these $Au_n(SR)_m$ nanoclusters should allow one to eventually correlate their catalytic performance with structure by combing theory and experiment. Such studies will ultimately identify the catalytically active sites on the particle, which has long been pursued in nanocatalysis. Apparently, with conventional polydisperse nanoparticles, the active site structure is difficult to investigate since the particle surface structure is unknown, while for $Au_{25}(SR)_{18}$, the atomic structure has been determined by X-ray crystallography,[11] and thus the catalytically active sites and reaction mechanism can be rationalized by combining experiment and theory.

In this work, we choose the $Au_{25}(SR)_{18}$ nanocluster (1 nm metal core) to investigate its catalytic activity for CO oxidation. The structure of $Au_{25}(SR)_{18}$ consists of a Au_{13} icosahedral core (which is relatively electron-rich) encapsulated by a nonclosed shell comprising 12 surface gold atoms (which are electron-deficient).[11,14,24] The low-coordinate Au atoms on the exterior shell of Au nanoparticles provide a favorable environment for the adsorption and activation of certain reactants;[25,26] hence, Au_{25} nanoclusters could be useful catalysts for certain reactions. Herein we demonstrate the high catalytic activity of $Au_{25}(SR)_{18}$ nanoclusters (in the supported form) for the CO oxidation reaction. Specifically, the $Au_{25}(SR)_{18}/CeO_2$ catalyst offers high catalytic performance in CO oxidation under mild conditions (*e.g.*, almost complete CO conversion at 80−100 °C). The $Au_n(SR)_m$ nanocluster catalysts hold promise in future real world applications.

RESULTS AND DISCUSSION

The synthesis of atomically precise $Au_{25}(SR)_{18}$ (R = CH_2CH_2Ph) nanoclusters follows a size-focusing method reported previously,[27] and the crystal structures of anionic and charge-neutral $Au_{25}(SR)_{18}$ nanoclusters have been determined by X-ray crystallography.[11,24] The oxide-supported catalysts were made by impregnation of metal oxide powder in a solution of $Au_{25}(SR)_{18}$ nanoclusters (see Experimental Section for details). After the clusters were adsorbed onto oxide surfaces, the cluster solution became clear. Then the supernatant was decanted, followed by vacuum drying of the $Au_{25}(SR)_{18}/MO_x$ catalyst at room temperature. The as-prepared catalyst is similar to the conventional supported catalysts in which the particles are deposited on bulk crystal substrates. Herein, we focus on the catalytic properties of $Au_{25}(SR)_{18}/MO_x$ for the CO oxidation reaction, including the effects of the supports, water vapor, and the pretreatment of catalysts in O_2 and N_2.

Effect of Supports and Pretreatment Conditions. It is well-known that the supports of Au catalysts have important influences on the catalytic performance.[2,5,6] We chose TiO_2, CeO_2, and Fe_2O_3 as supports for $Au_{25}(SR)_{18}$. According to our measurements, the plain TiO_2 and CeO_2 supports were essentially inert below 200 °C, while Fe_2O_3 shows some activity for CO oxidation above 120 °C. The reducibility of metal oxides under CO atmosphere is generally believed to contribute to the catalytic activity. Below, we discuss the catalytic properties of $Au_{25}(SR)_{18}$ nanoclusters supported on TiO_2, CeO_2, and Fe_2O_3.

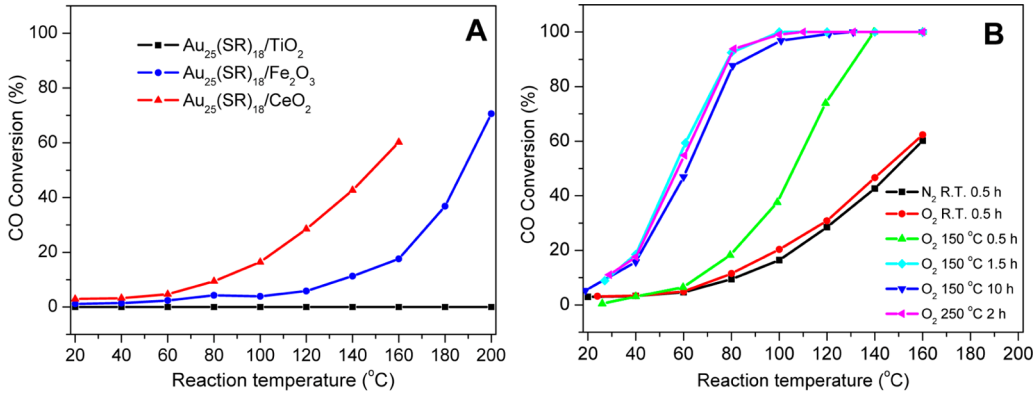

Figure 1. (A) Reaction temperature dependence of CO conversion over $Au_{25}(SR)_{18}/MO_x$ catalysts. Pretreatment condition: N_2 at room temperature (rt) for 0.5 h. Reaction conditions: GHSV = 7500 mL g^{-1} h^{-1}, catalyst = 0.1 g. (B) Reaction temperature dependence of CO conversion over $Au_{25}(SR)_{18}/CeO_2$ catalyst after different pretreatments. GHSV = 7500 mL g^{-1} h^{-1}.

The various oxide-supported $Au_{25}(SR)_{18}$ nanocluster catalysts exhibit drastic effects in CO oxidation (Figure 1A). Unexpectedly, the $Au_{25}(SR)_{18}/TiO_2$ catalyst shows almost no catalytic activity, even up to 200 °C, which is strikingly different from conventional Au/TiO_2 catalysts that exhibit extraordinary activity as reported by many groups.[5,6,28] The $Au_{25}(SR)_{18}/Fe_2O_3$ catalyst exhibits some activity above 120 °C, but the activity is actually lower than that of *plain* Fe_2O_3 support under the same reaction conditions. Among the three types of catalysts, $Au_{25}(SR)_{18}/CeO_2$ gave rise to the highest CO oxidation conversion and achieved 50% conversion of CO at ~150 °C (Figure 1A).

Interestingly, we discovered that thermal pretreatment of $Au_{25}(SR)_{18}/CeO_2$ in O_2 can significantly boost its catalytic activity (Figure 1B). Different temperatures were tested for the O_2 pretreatment process. The catalyst pretreated with O_2 for 0.5 h at rt exhibited a slight increase in activity than that pretreated by N_2 at rt (Figure 1B, red and black profiles). However, O_2 pretreatment at 150 °C for 0.5 h dramatically increased the catalyst's activity (Figure 1B, green profile). Moreover, as the 150 °C O_2 pretreatment time increased from 0.5 to 1.5 h, the CO conversion further dramatically increased from 18.2 to 92.4% at reaction temperature (T_{rxn}) = 80 °C. Prolonged pretreatment from 1.5 to 10 h at 150 °C, however, did not lead to further increase in catalytic activity, indicating that thermal pretreatment in O_2 for 1.5 h is sufficient. We also tested higher pretreatment temperatures (T_{pre}, 250 °C), but no further increase in activity was observed as T_{pre} was increased from 150 to 250 °C. On the other hand, thermal pretreatment of the $Au_{25}(SR)_{18}/CeO_2$ catalyst in N_2 seems to be ineffective.

A question arises naturally: Does the thermal O_2 pretreatment process remove the surface thiolate ligands on Au_{25} nanoclusters? To address this, we performed thermogravimetric analysis (TGA) of $Au_{25}(SR)_{18}$ in pure O_2 atmosphere (~100 mL/min) (Figure 2). TGA shows that thiolates start to desorb at ~200 °C. The onset temperature is independent of atmosphere (*i.e.*, O_2, N_2, and air). Therefore, during the 150 °C O_2 pretreatment, the ligands should remain on the Au_{25} nanoclusters. Moreover, since the CO oxidation reaction temperature is only up to 160 °C (Figure 1B), the CO oxidation process should be catalyzed by ligands-on, *intact* $Au_{25}(SR)_{18}$ nanoclusters. Further evidence is presented in the mechanistic discussion (*vide infra*). This is important for gaining insight into the structure–activity relationship.

The result of CO oxidation catalyzed by intact $Au_{25}(SR)_{18}/CeO_2$ catalyst is quite remarkable compared to previous work[4,29–31] in which surface thiolate ligands were completely removed by a high-temperature calcination process (typically at 300–375 °C); note that the latter temperature is already above the thiolate ligand desorption temperature of $Au_n(SR)_m$ nanoclusters.

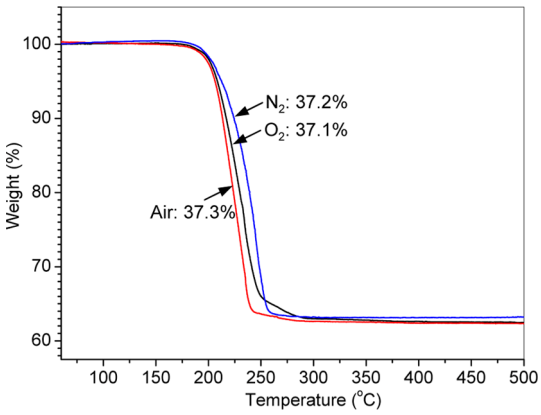

Figure 2. TGA profiles of $Au_{25}(SR)_{18}$ nanoclusters in various atmospheres.

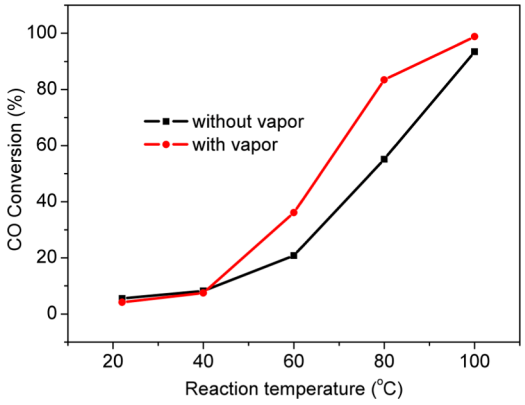

Figure 3. Effect of water vapor on the CO conversion over $Au_{25}(SR)_{18}/CeO_2$ catalyst pretreated by O_2 at 150 °C for 2 h; GHSV = 15 000 mL g^{-1} h^{-1}.

Our results imply that the ligands do not inhibit the activity of the catalyst as we thought initially, at least in the CO oxidation reaction.

Effect of Water Vapor. For nanogold-catalyzed CO oxidation, another distinct and well-known effect pertains to moisture (*i.e.*, water vapor) in the feed stock.[32–35] The observed effects of water vapor on the catalyst activity include enhancement,[32,33] suppression,[34] or no effect.[35] To investigate the moisture effect on the $Au_{25}(SR)_{18}/CeO_2$ catalyst's performance, we introduced water vapor into the reaction gas mixture. The catalyst was first pretreated in O_2 at 150 °C for 2 h according to the above determined pretreatment conditions. The $CO/O_2/He$ feed gas was first passed through a water saturator at ambient temperature before being introduced into the fixed bed reactor. The CO conversion was measured as a function of reaction temperature (Figure 3); note that, in this test, the GHSV was increased from 7500 (condition in Figure 1) to 15 000 mL g^{-1} h^{-1}. The CO conversion was also compared to the case of *dry* feed gas (without passing through the water saturator) (Figure 3). This comparison clearly shows that CO conversion for the case of wet feed gas is higher than the case of dry feed gas, especially between the temperature range of 60 to

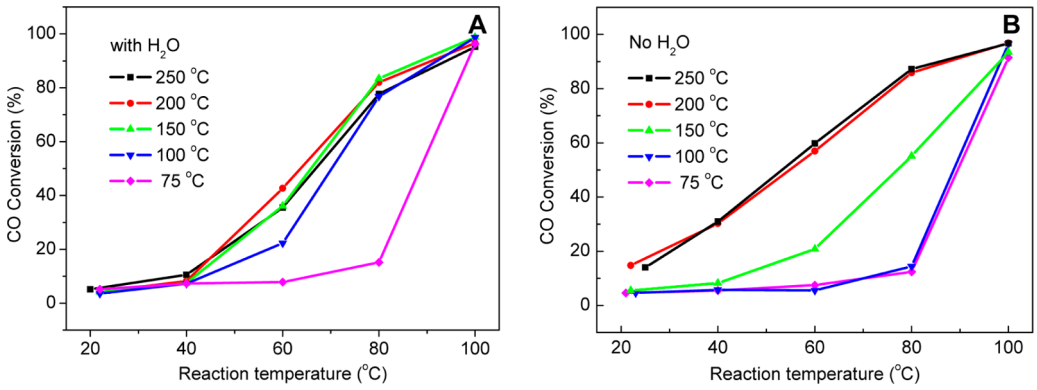

Figure 4. Effect of water vapor on CO conversion over various pretreated $Au_{25}(SR)_{18}/CeO_2$ catalysts under different pretreatment temperatures: (A) feed gases with water vapor and (B) without vapor. Pretreatment conditions: in O_2 for 2 h and the T_{pre} is as shown in the figure. Reaction: GHSV = 15 000 mL g^{-1} h^{-1}, 0.1 g supported catalyst.

80 °C (Figure 3), which implies a promoting effect of vapor on CO oxidation over $Au_{25}(SR)_{18}/CeO_2$. This effect is consistent with most work about Au/MO_x catalysts reported previously.

The influence of water vapor on the catalytic activity was further investigated for $Au_{25}(SR)_{18}/CeO_2$ catalysts pretreated by O_2 at different temperatures. According to the TGA result of $Au_{25}(SR)_{18}$ nanocluster (Figure 2), $Au_{25}(SR)_{18}$ starts to lose weight at *ca.* 200 °C due to thermal desorption of thiolate ligands, and the process finishes at ~250 °C. Therefore, we chose five different pretreatment temperatures, T_{pre} = 75, 100, 150, 200, and 250 °C, to study the variation of catalytic properties of $Au_{25}(SR)_{18}$ before and after ligand loss. In a typical measurement for a pretreatment temperature, the CO conversion over $Au_{25}(SR)_{18}/CeO_2$ was first measured in the reaction temperature range from rt to 100 °C (note that CO is completely converted at ~100 °C; hence, higher reaction temperatures were not pursued). Then the feed gas was passed through a water saturator, and similar measurements were done. The results for the presence/absence of water vapor are, shown in Figure 4A,B, respectively. The results indicate that the 100 and 150 °C pretreatment temperatures exhibit most drastic effects for the presence/absence of water vapor; for example, in the case of T_{pre} = 100 °C, the catalyst offers 50% conversion of CO at reaction temperature of ~88 °C with dry feed gas (Figure 4B, blue) but 70 °C in the presence of vapor (Figure 4A, blue). The results indicate that water vapor promotes the catalyst's activity at relatively low temperatures, while at higher reaction temperatures (T_{rxn} > 100 °C), no distinct effect of vapor was observed since CO is already completely converted regardless the presence of vapor. Similarly, in the case of T_{pre} = 150 °C, the 50% conversion temperatures are 77 and 65 °C for the absence and presence of vapor, respectively, indicating a distinct promotion effect of water vapor. On the other hand, for the catalysts pretreated at higher temperatures (*e.g.*, 200 and 250 °C), the addition of water vapor to the feed gas did not exert any beneficial effect on CO oxidation; rather, water vapor slightly inhibits the catalytic activity, evidenced by the increase in the reaction temperature for 50% CO conversion (Table 1).

TABLE 1. Reaction Temperature for 50% CO Conversion in the Presence/Absence of Vapor

	T_{rxn} for 50% CO conversion, with H_2O	T_{rxn} for 50% CO conversion, no H_2O
catalyst pretreated at 75 °C	89	90
catalyst pretreated at 100 °C	70	88
catalyst pretreated at 150 °C	65	77
catalyst pretreated at 200 °C	63	55
catalyst pretreated at 250 °C	67	53

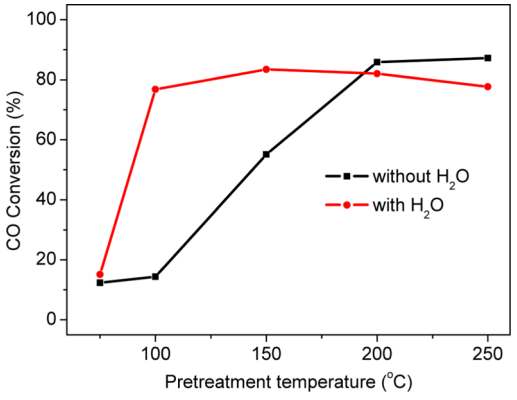

Figure 5. CO conversion at T_{rxn} = 80 °C for the $Au_{25}(SR)_{18}/CeO_2$ catalyst pretreated at different temperatures (red, with water vapor; black, without vapor). GHSV = 15 000 mL g^{-1} h^{-1}.

In consideration of the possible state of $Au_{25}(SR)_{18}/CeO_2$ at different pretreatment temperatures, we conclude that $Au_{25}(SR)_{18}/CeO_2$ is more suitable than conventional supported nanogold catalysts for CO oxidation with the *wet* feed gas. This is also supported by the results shown in Figure 5, in which one can clearly see that the 100 °C O_2-pretreated $Au_{25}(SR)_{18}/CeO_2$ catalyst gives rise to ~80% CO conversion at T_{rxn} = 80 °C when water vapor is present in the feed

gas. Pretreatment of the catalyst at 150 °C also leads to a quite large increase in CO conversion at 80 °C (note: comparing the red and black profiles at T_{pre} = 150 °C), while further higher temperatures (*e.g.*, 200 to 250 °C, above the onset of thiolate desorption) do not show such a promoting effect of vapor as discussed above.

Insight into the Catalytic Mechanism. The above results clearly demonstrate the significant effect of thermal O_2 pretreatment (*e.g.*, 150 °C for 1.5−2 h) on the activity of the $Au_{25}(SR)_{18}/CeO_2$ catalyst. Interestingly, such a drastic effect was not observed in the $Au_{25}(SR)_{18}/TiO_2$ system. For the latter system, we performed thermal pretreatments even up to 250 °C in O_2 atmosphere, but only a slight increase in catalytic activity was observed (*i.e.*, increased from ~0 (see Figure 1A) to 8.8% CO conversion (without H_2O vapor in the feed gas) or 16.7% (with vapor in the feed gas) at 120 °C (catalytic reaction temperature)).

As discussed above, the organic ligands on the catalyst should remain when pretreated at 150 °C in O_2 according to the TGA results (Figure 2). The weight loss amounts under various atmospheres are indeed the same: weight loss of 37.1 wt % under O_2, 37.3 wt % under air, and 37.2 wt % under N_2. Thus, O_2 does not burn off organic ligands on the cluster surface during the 150 °C pretreatment process, albeit burning might occur at higher temperatures (>200 °C; see the TPO-MS analysis below). We have also performed N_2 pretreatment at 150 °C to compare with the O_2 pretreatment at the same temperature, but no significant effect in enhancing catalytic activity was observed. Then, an interesting question is what O_2 does to the catalyst during the 150 °C thermal pretreatment process.

In order to gain insight into the activation mechanism of $Au_{25}(SR)_{18}/CeO_2$ catalyst *via* O_2 pretreatment, we carried out temperature-programmed oxidation in a O_2 atmosphere (O_2-TPO) experiments, in which the signals of O_2 consumption, H_2O and CO_2 generation were monitored by mass spectrometry. The pure CeO_2 powders and CH_2Cl_2-impregnated CeO_2 were also tested together with the $Au_{25}(SR)_{18}/CeO_2$ catalyst; note that the CH_2Cl_2-impregnated CeO_2 sample dried before TPO experiments was included because CH_2Cl_2 was used as the solvent during the deposition process of $Au_{25}(SR)_{18}$ onto CeO_2. From Figure 6A, it can be seen that O_2 consumption for $Au_{25}(SR)_{18}/CeO_2$ started to appear around 150 °C and a peak centered at ~200 °C was observed, but no O_2 consumption was found in plain CeO_2 and CH_2Cl_2-impregnated CeO_2 (Figure 6A). The H_2O signals were observed at ~200 °C and above (Figure 6B), which were ascribed to H_2O desorption from the catalyst surface (for plain CeO_2 and CH_2Cl_2-impregnated CeO_2), while the case of $Au_{25}(SR)_{18}/CeO_2$ may also involve O_2 burning of desorbed ligands at >200 °C, evidenced by a much larger CO_2 peak at ~220 °C than the cases of plain CeO_2 and CH_2Cl_2-impregnated CeO_2 (Figure 6C). It is worth noting that in all three samples a low-temperature CO_2 peak

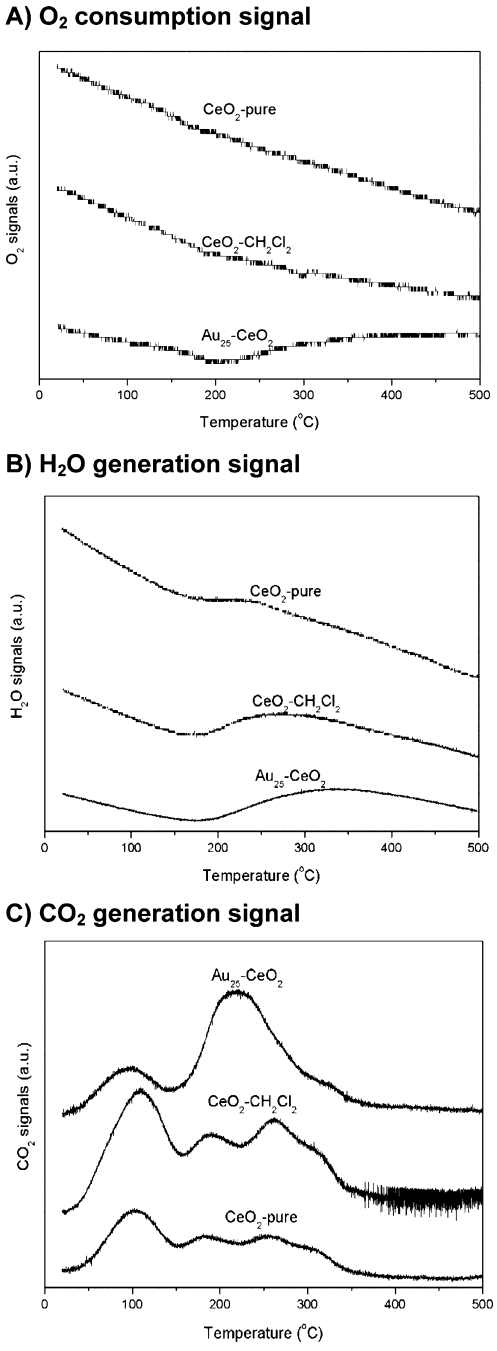

Figure 6. MS signals of TPO profiles of $Au_{25}(SR)_{18}/CeO_2$ catalyst, (A) O_2, (B) H_2O, and (C) CO_2. Three samples ($Au_{25}(SR)_{18}/CeO_2$, pure CeO_2, and CH_2Cl_2-impregnated CeO_2 support) were tested in TPO-MS experiments.

(centered at ~100 °C) was found (Figure 6C), which is due to the known fact that CeO_2 powders capture CO_2 in air but not due to burning of the thiolate ligand of $Au_{25}(SR)_{18}$ clusters since no corresponding H_2O peak was observed at ~100 °C (Figure 6B). Taken together, the H_2O and CO_2 generation processes above 200 °C are not relevant to the 150 °C O_2 pretreatment of the catalyst; instead, the pretreatment process should involve adsorption and activation of O_2 on the catalyst, and upon the generation of such active oxygen

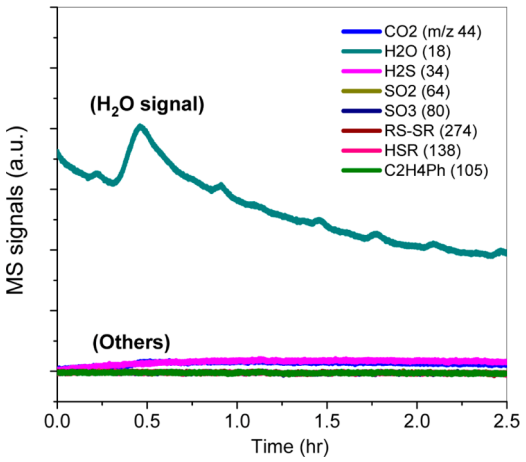

Figure 7. TGA-MS analysis of the 150 °C thermal pretreatment of the $Au_{25}(SR)_{18}/CeO_2$ catalyst in air. No desorption of thiolate ligands or burning of ligands into SO_2/SO_3 was detected.

species, the CO oxidation reaction can proceed smoothly with high catalytic conversion.

The above analyses clearly indicate that thermal activation of $Au_{25}(SR)_{18}/CeO_2$ for high catalytic activity is not due to ligand desorption (which occurs at >200 °C). While holding the catalyst temperature at 150 °C, TGA analysis showed no weight loss of the $Au_{25}(SR)_{18}/CeO_2$ catalyst during the 2 h isothermal process in O_2, thus the desorption of thiolate ligands is determined by thermodynamics (i.e. the temperature must be >200 °C to desorb thiolates), rather than by kinetics. To further confirm that thiolate ligands are not desorbed in the 150 °C pretreatment process, we have performed TGA-MS analysis to monitor if any sulfur-containing compound is emitted. A mass spectrometer monitored simultaneously multiple signals, including *m/z* 34 for H_2S, *m/z* 64 for SO_2, *m/z* 80 for SO_3, *m/z* 274 for disulfide $PhC_2H_4S\text{-}SC_2H_4Ph$, *m/z* 138 for HSC_2H_4Ph, *m/z* 105 for fragment C_2H_4Ph, as well as H_2O (*m/z* 18) and CO_2 (*m/z* 44), but no emissions of thiol, disulfide, or other sulfur-containing compounds was detected, except a H_2O peak since oxides typically adsorb moisture (Figure 7). Thus, our conclusion is further confirmed. One may wonder whether the thiolate ligand is subjected to some change at 150 °C; this is also ruled out by a separate study.[36] We previously characterized $Au_{25}(SR)_{18}$ nanoclusters after thermal treatment at different temperatures by nuclear magnetic resonance (NMR) spectroscopy. NMR analyses demonstrated that the thiolate ligands remain *intact* up to 180−190 °C (close to the onset temperature of thiolate desorption), evidenced by the identical NMR signals from the surface thiolate ligands before and after thermal treatment. Therefore, the 150 °C pretreatment of the $Au_{25}(SR)_{18}/CeO_2$ catalyst in O_2 or N_2 should not lead to any changes to the ligand and the Au_{25} core. Of note, the charge state of $Au_{25}(SR)_{18}$ may be changed from $q = -1$ to 0 after interaction with

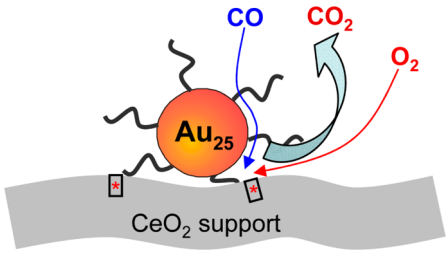

Scheme 1. Proposed model for CO oxidation at the perimeter sites of $Au_{25}(SR)_{18}/CeO_2$ catalyst.

O_2, but it is the *Au_{25} core*, rather than the *thiolate* ligands, that donates an electron to O_2.[24] X-ray crystallography confirmed that the structure of $[Au_{25}(SR)_{18}]^0$ is the same as that of $[Au_{25}(SR)_{18}]^-$.[24] The Au_{25} core charge states were found to cause distinct shifts of the NMR peaks, thus, the previous NMR studies[36] were done in N_2 (as opposed to O_2) to avoid any charge state change; nevertheless, our conclusion that the $Au_{25}(SR)_{18}$ remains intact should be valid regardless of the atmosphere (N_2 or O_2) in the pretreatment conditions. X-ray spectroscopic analysis is underway, which will provide further insight.

Although further work is still needed to reveal details of the catalytic mechanism, we attribute the significant effect of 100−150 °C O_2 pretreatment on the catalyst to the formation of an active surface oxygen species, while such an oxygen species was not created during the N_2 pretreatment under comparable conditions since N_2 is inert; hence, N_2 pretreatment is not as effective as O_2 pretreatment. This analysis raises another intriguing question: where is the active oxygen species located? The drastic effect of various oxide supports (Figure 1A) indicates that the *interfacial* interaction between gold clusters and the support is a key factor. While the mechanism for the interfacial interaction of gold with oxide supports needs detailed analysis by X-ray photoelectron (XPS) and X-ray absorption spectroscopy (XAS),[37] we believe that the interface between $Au_{25}(SR)_{18}$ and CeO_2 should constitute the catalytic active sites (Scheme 1) with reasons as follows.

Firstly, the interfacial oxidation of CO by some active oxygen species is consistent with the drastic effects of supports as reflected in Figure 1A. CeO_2 is well-known to be capable of activating O_2 molecules[38] due to the rich oxygen vacancies in CeO_2.[39] If the external surface of $Au_{25}(SR)_{18}$ were where CO oxidation occur, then the drastic support effect would be hard to explain. Secondly, thermal O_2 pretreatment of the catalyst indicates that the 100−150 °C range is most effective for boosting the catalyst's activity (see Figure 1B and Figure 5). Should the external surface of Au_{25} particles be responsible for CO oxidation, then pretreatment at >200 °C would largely increase catalytic activity since ligands are desorbed at >200 °C, but no further increase in catalytic activity was observed

at all the reaction temperatures (20−100 °C) for the catalyst pretreated at higher temperatures than 200 °C (Figure 1B). Lastly, the promoting effect of water vapor also tends to occur more reasonably at the $Au_{25}(SR)_{18}/CeO_2$ interface, rather than on the external surface of $Au_{25}(SR)_{18}$ since the phenylethanethiolate ligand is hydrophobic.

Overall, our results imply that the interface between $Au_{25}(SR)_{18}$ and the oxide support, more specifically, the perimeter of the $Au_{25}(SR)_{18}/CeO_2$ interface, should be the catalytically active centers for CO oxidation. This supports the recent view on CO oxidation discussed by Haruta.[40] In the $Au_{25}(SR)_{18}/CeO_2$ catalyst, the perimeter sites are apparently strongly affected by thermal O_2 pretreatment, and the active oxygen species (presumably some peroxyl or hydroperoxyl species) are adsorbed at such perimeter sites and initiate the CO oxidation reaction. In the case of supported, bare gold particles (as opposed to our ligands-on Au particles), Guzman *et al.* observed reactive oxygen in the form of surface superoxide and peroxide species in CO oxidation.[41] Very recently, Kim *et al.*[42] discussed three CO oxidation mechanisms on CeO_2-supported Au nanoparticles on the basis of DFT calculations, including (1) CO oxidation by coadsorbed O_2, (2) by lattice oxygen in CeO_2, and (3) by O_2 bound to a $Au-Ce^{3+}$ anchoring site. While all these works refer to bare Au particles, in our case, the Au_{25} particles are capped by thiolate ligands and there are possibly some major differences between the two systems. For future work, we hope to probe the $Au_{25}(SR)_{18}/CeO_2$ interface, including the possible charge transfer between $Au_{25}(SR)_{18}$ and CeO_2, the potential changes in the coordination environment of surface gold atoms after 150 °C O_2 pretreatment, and more details about the activation process of $Au_{25}(SR)_{18}/CeO_2$. By correlating with the atomic packing structure of $Au_{25}(SR)_{18}$, we believe that future experiment and theory will reveal the fundamental mechanisms of CO and O_2 activation and the detailed surface reactions.

CONCLUSION

In summary, we have investigated the CO catalytic oxidation by O_2 over TiO_2-, CeO_2-, and Fe_2O_3-supported $Au_{25}(SR)_{18}/MO_x$ catalysts. The well-defined catalysts prepared by deposition of solution phase, atomically precise $Au_{25}(SR)_{18}$ nanoclusters onto oxide supports provide some unique opportunities for probing the fundamental aspects of the catalytic reaction. Among the three supported catalysts, the $Au_{25}(SR)_{18}/CeO_2$ system exhibits the highest activity. Adding water vapor to the feed gas benefits the CO conversion, especially at mild reaction temperatures (60−80 °C). A particularly interesting result is the significant increase in catalytic activity of the O_2-pretreated $Au_{25}(SR)_{18}/CeO_2$ catalyst at 100−150 °C for 1.5−2 h. The very low activity of $Au_{25}(SR)_{18}/TiO_2$ (even after 250 °C pretreatment in O_2 atmosphere) is a surprise and remains to be elucidated in future work. Our results imply that the CO oxidation by O_2 is catalyzed by intact $Au_{25}(SR)_{18}$ nanoclusters supported on CeO_2. The interface of $Au_{25}(SR)_{18}/CeO_2$ is critical for the catalytic reaction, and O_2 adsorption and conversion to certain active species (possibly peroxyl or hydroperoxyl species) is rationalized to occur at the perimeter sites of the catalyst during the 150 °C O_2 pretreatment process. The issue of the perimeter Au sites *versus* low-coordinated corner Au sites being the active sites is particularly intriguing in gold catalysis.[43] Since the atomic packing structure of $Au_{25}(SR)_{18}$ is known, future work should allow for gaining deep insight into the catalytic mechanism, including identification of the exact form of the active oxygen species and the mechanism for CO and O_2 activation and detailed surface reactions. We believe that the nanocluster catalysts, as a new type of well-defined nanocatalyst, hold promise in fundamental studies of the catalytic mechanisms by correlating their catalytic performance with atomic structures.[44−46]

EXPERIMENTAL SECTION

Preparation of $Au_n(SR)_m/MO_x$ Catalysts. For the synthesis of $Au_{25}(SR)_{18}$ nanoclusters, a kinetically controlled, size-focusing approach was used.[27] The structure of $Au_{25}(SR)_{18}$ has been reported in our previous work.[11] Supported $Au_n(SR)_m/MO_x$ (including TiO_2, CeO_2, Fe_2O_3) catalysts were prepared as follows: 500 mg of the oxide support (in powder form) was impregnated by soaking the powders in a solution of 5−10 mg $Au_n(SR)_m$ nanoclusters in CH_2Cl_2 (*ca.* 10 mL) in a sealed vial for 24 h, followed by drying; note that no calcination was performed. The TiO_2 support uses commercial Degussa P-25; CeO_2 is prepared by coprecipitation of $(NH_4)_2Ce(NO_3)_6$ and $(NH_4)_2CO_3$, followed by calcination at 500 °C; Fe_2O_3 is obtained by coprecipitation of $Fe(NO_3)_3$ and Na_2CO_3, followed by calcinations at 400 °C. The $Au_n(SR)_m/MO_x$ catalysts used in the activity tests are 1 wt % $Au_{25}(SR)_{18}/TiO_2$, 2% $Au_{25}(SR)_{18}/CeO_2$, and 2 wt % $Au_{25}(SR)_{18}/Fe_2O_3$ (the weight percentage refers to the ligand-protected form of the clusters).

Catalytic Activity Test for CO Oxidation. The supported $Au_n(SR)_m/MO_x$ catalyst activity was tested in a fixed bed, continuous flow quartz reactor (8 mm inside diameter) under ambient pressure and with gas hourly space velocity (GHSV) ranging from 7500−15 000 mL g^{-1} h^{-1}. Prior to the reaction, the $Au_n(SR)_m/MO_x$ catalyst was pretreated at given temperatures for 2 h in a pretreatment atmosphere unless otherwise noted. In a typical experiment, 50−100 mg of $Au_n(SR)_m/MO_x$ catalyst was heated to the pretreatment temperature at a heating rate of 5 °C/min in an O_2 flow (30 mL/min). The catalyst was kept at that temperature for 2 h and then spontaneously cooled to ambient temperature before switching to the reactant gas mixture consisting of 1.67% CO, 3.33% O_2, and 95% He. The flows of inlet gases were controlled by mass-flow controllers

(MFC). The catalyst was conditioned for 0.5 h in this mixture at ambient temperature before the products were analyzed by an online gas chromatograph (Shimadzu, GC-8A), which was equipped with a carbon molecular sieve column (TDX-01, Dalian Zhonghuida Scientific Instrument Co. Ltd.) and a thermal conductivity detector (TCD). Analogous measurements were performed in 20 °C intervals between 20 and 200 °C reaction temperature. The reaction temperature was controlled by a programmable temperature controller and detected by a movable thermocouple inside the catalyst bed.

Catalyst Characterization. Thermogravimetric analysis (TGA) was performed on TGA50 analyzer (Shimadzu) under different atmosphere (N_2, O_2, and air). The oxygen temperature-programmed oxidation (O_2-TPO) analysis was carried out using a homemade setup equipped with an online mass analysis system (Pfeiffer OmniStar mass spectrometer). Typically, 40 mg of catalyst was initially pretreated in Ar at room temperature for 30 min, then the oxidizing agent (5 vol % O_2/Ar, 30 mL/min) was introduced, and the sample was tested from 20 to 500 °C at a ramp rate of 5 °C/min. O_2 (m/z = 32), H_2O (m/z = 18), and CO_2 (m/z = 44) produced were recorded as functions of temperature. The 150 °C pretreatment process in a O_2 atmosphere was also monitored by mass spectrometry, including both the temperature ramp process (for 0.5 h) and the subsequent isothermal process at 150 °C (for 2 h); no ligand desorption was observed.

Conflict of Interest: The authors declare no competing financial interest.

Acknowledgment. The authors thank Prof. Wenzhao Li and Prof. Yanxin Chen for helpful discussions. R.J. acknowledges research support by the Air Force Office of Scientific Research under AFOSR Award No. FA9550-11-1-9999 (FA9550-11-1-0147).

REFERENCES AND NOTES

1. Haruta, M.; Kobayashi, T.; Sano, H.; Yamada, N. Novel Gold Catalysts for the Oxidation of Carbon-Monoxide at a Temperature Far Below 0-Degrees-C. *Chem. Lett.* **1987**, 405–408.
2. Haruta, M.; Yamada, N.; Kobayashi, T.; Iijima, S. Gold Catalysts Prepared by Coprecipitation for Low-Temperature Oxidation of Hydrogen and of Carbon Monoxide. *J. Catal.* **1989**, *115*, 301–309.
3. Valden, M.; Lai, X.; Goodman, D. W. Onset of Catalytic Activity of Gold Clusters on Titania with the Appearance of Nonmetallic Properties. *Science* **1998**, *281*, 1647–1650.
4. Jia, C.-J.; Liu, Y.; Bongard, H.; Schuth, F. Very Low Temperature CO Oxidation over Colloidally Deposited Gold Nanoparticles on $Mg(OH)_2$ and MgO. *J. Am. Chem. Soc.* **2010**, *132*, 1520–1522.
5. Kung, M. C.; Davis, R. J.; Kung, H. H. Understanding Au-Catalyzed Low-Temperature CO Oxidation. *J. Phys. Chem. C* **2007**, *111*, 11767–11775.
6. Bond, G. C.; Louis, C.; Thompson, D. T. *Catalysis by Gold*; Imperial College Press: London, 2006.
7. Gao, F.; Wood, T.; Goodman, D. The Effects of Water on CO Oxidation over TiO_2 Supported Au Catalysts. *Catal. Lett.* **2010**, *134*, 9–12.
8. Jin, R.; Qian, H.; Wu, Z.; Zhu, Y.; Zhu, M.; Mohanty, A.; Garg, N. Size Focusing: A Methodology for Synthesizing Atomically Precise Gold Nanoclusters. *J. Phys. Chem. Lett.* **2010**, *1*, 2903–2910.
9. Wu, Z.; MacDonald, M. A.; Chen, J.; Zhang, P.; Jin, R. Kinetic Control and Thermodynamic Selection in the Synthesis of Atomically Precise Gold Nanoclusters. *J. Am. Chem. Soc.* **2011**, *133*, 9670–9673.
10. Shichibu, Y.; Negishi, Y.; Tsunoyama, H.; Kanehara, M.; Teranishi, T.; Tsukuda, T. Extremely High Stability of Glutathionate-Protected Au_{25} Clusters Against Core Etching. *Small* **2007**, *3*, 835–839.
11. Zhu, M.; Aikens, C. M.; Hollander, F. J.; Schatz, G. C.; Jin, R. Correlating the Crystal Structure of A Thiol-Protected Au_{25} Cluster and Optical Properties. *J. Am. Chem. Soc.* **2008**, *130*, 5883–5885.
12. Qian, H.; Zhu, Y.; Jin, R. Size-Focusing Synthesis, Optical and Electrochemical Properties of Monodisperse $Au_{38}(SC_2H_4Ph)_{24}$ Nanoclusters. *ACS Nano* **2009**, *3*, 3795–3803.
13. Qian, H.; Eckenhoff, W. T.; Zhu, Y.; Pintauer, T.; Jin, R. Total Structure Determination of Thiolate-Protected Au_{38} Nanoparticles. *J. Am. Chem. Soc.* **2010**, *132*, 8280–8281.
14. Zhu, M.; Aikens, C. M.; Hendrich, M. P.; Gupta, R.; Qian, H.; Schatz, G. C.; Jin, R. Reversible Switching of Magnetism in Thiolate-Protected Au_{25} Superatoms. *J. Am. Chem. Soc.* **2009**, *131*, 2490–2492.
15. Zhu, M.; Qian, H.; Meng, X.; Jin, S.; Wu, Z.; Jin, R. Chiral Au_{25} Nanospheres and Nanorods: Synthesis and Insight into the Origin of Chirality. *Nano Lett.* **2011**, *11*, 3963–3969.
16. Qian, H.; Zhu, Y.; Jin, R. Atomically Precise Gold Nanocrystal Molecules with Surface Plasmon Resonance. *Proc. Natl. Acad. Sci. U.S.A.* **2012**, *109*, 696–700.
17. Tsukuda, T.; Tsunoyama, H.; Sakurai, H. Aerobic Oxidations Catalyzed by Colloidal Nanogold. *Chem. Asian J.* **2011**, *6*, 736–748.
18. Liu, Y.; Tsunoyama, H.; Akita, T.; Xie, S.; Tsukuda, T. Aerobic Oxidation of Cyclohexane Catalyzed by Size-Controlled Au Clusters on Hydroxyapatite: Size Effect in the Sub-2 nm Regime. *ACS Catal.* **2011**, *1*, 2–6.
19. Zhu, Y.; Qian, H.; Zhu, M.; Jin, R. Thiolate-Protected Au_n Nanoclusters as Catalysts for Selective Oxidation and Hydrogenation Processes. *Adv. Mater.* **2010**, *22*, 1915–1920.
20. Negishi, Y.; Tsunoyama, H.; Suzuki, M.; Kawamura, N.; Matsushita, M. M.; Maruyama, K.; Sugawara, T.; Yokoyama, T.; Tsukuda, T. X-ray Magnetic Circular Dichroism of Size-Selected, Thiolated Gold Clusters. *J. Am. Chem. Soc.* **2006**, *128*, 12034–12035.
21. MacDonald, M. A.; Chevrier, D. M.; Zhang, P.; Qian, H.; Jin, R. The Structure and Bonding of $Au_{25}(SR)_{18}$ Nanoclusters from EXAFS: The Interplay of Metallic and Molecular Behavior. *J. Phys. Chem. C* **2011**, *115*, 15282–15287.
22. Sakai, N.; Tatsuma, T. Photovoltaic Properties of Glutathione-Protected Gold Clusters Adsorbed on TiO_2 Electrodes. *Adv. Mater.* **2010**, *22*, 3185–3188.
23. Kogo, A.; Sakai, N.; Tatsuma, T. Photocatalysis of Au_{25}-Modified TiO_2 under Visible and Near Infrared Light. *Electrochem. Commun.* **2010**, *12*, 996–999.
24. Zhu, M.; Eckenhoff, W. T.; Pintauer, T.; Jin, R. Conversion of Anionic $[Au_{25}(SCH_2CH_2Ph)_{18}]^-$ Cluster to Charge Neutral Cluster *via* Air Oxidation. *J. Phys. Chem. C* **2008**, *112*, 14221–14224.
25. Zhu, Y.; Wu, Z.; Gayathri, C.; Qian, H.; Gil, R. R.; Jin, R. Exploring Stereoselectivity of Au_{25} Nanoparticle Catalyst for Hydrogenation of Cyclic Ketone. *J. Catal.* **2010**, *271*, 155–160.
26. Corma, A.; Boronat, M.; Gonzalez, S.; Illas, F. On the Activation of Molecular Hydrogen by Gold: A Theoretical Approximation to the Nature of Potential Active Sites. *Chem. Commun.* **2007**, 3371–3373.
27. Zhu, M.; Lanni, E.; Garg, N.; Bier, M. E.; Jin, R. Kinetically Controlled, High-Yield Synthesis of Au_{25} Clusters. *J. Am. Chem. Soc.* **2008**, *130*, 1138–1139.
28. Haruta, M.; Tsubota, S.; Kobayashi, T.; Kageyama, H.; Genet, M. J.; Delmon, B. Low-Temperature Oxidation of CO over Gold Supported on TiO_2, α-Fe_2O_3, and Co_3O_4. *J. Catal.* **1993**, *144*, 175–192.
29. Yin, H.; Ma, Z.; Chi, M.; Dai, S. Heterostructured Catalysts Prepared by Dispersing Au@Fe_2O_3 Core–Shell Structures on Supports and Their Performance in CO Oxidation. *Catal. Today* **2011**, *160*, 87–95.
30. Wanjala, B. N.; Luo, J.; Fang, B.; Mott, D.; Zhong, C.-J. Gold–Platinum Nanoparticles: Alloying and Phase Segregation. *J. Mater. Chem.* **2011**, *21*, 4012–4020.
31. Hickey, N.; Arneodo Larochette, P.; Gentilini, C.; Sordelli, L.; Olivi, L.; Polizzi, S.; Montini, T.; Fornasiero, P.; Pasquato, L.; Graziani, M. Monolayer Protected Gold Nanoparticles on Ceria for an Efficient CO Oxidation Catalyst. *Chem. Mater.* **2007**, *19*, 650–651.

32. Park, E. D.; Lee, J. S. Effects of Pretreatment Conditions on CO Oxidation over Supported Au Catalysts. *J. Catal.* **1999**, *186*, 1–11.
33. Cunningham, D. A. H.; Vogel, W.; Haruta, M. Negative Activation Energies in CO Oxidation over an Icosahedral Au/$Mg(OH)_2$ Catalyst. *Catal. Lett.* **1999**, *63*, 43–47.
34. Bollinger, M. A.; Vannice, M. A. A Kinetic and DRIFTS Study of Low-Temperature Carbon Monoxide Oxidation over Au-TiO_2 Catalysts. *Appl. Catal., B* **1996**, *8*, 417–443.
35. Liu, H.; I. Kozlov, A.; P. Kozlova, A.; Shido, T.; Iwasawa, Y. Active Oxygen Species and Reaction Mechanism for Low-Temperature CO Oxidation on an Fe_2O_3-Supported Au Catalyst Prepared from $Au(PPh_3)(NO_3)$ and As-Precipitated Iron Hydroxide. *Phys. Chem. Chem. Phys.* **1999**, *1*, 2851–2860.
36. Wu, Z.; Jin, R. Stability of the Two Au-S Binding Modes in $Au_{25}(SG)_{18}$ Nanoclusters Probed by NMR and Optical Spectroscopy. *ACS Nano* **2009**, *3*, 2036–2042.
37. MacDonald, M. A.; Zhang, P.; Qian, H.; Jin, R. Site-Specific and Size-Dependent Bonding of Compositionally Precise Gold Thiolate Nanoparticles from X-ray Spectroscopy. *J. Phys. Chem. Lett.* **2010**, *1*, 1821–1825.
38. Imagawa, H.; Suda, A.; Yamamura, K.; Sun, S. Monodisperse CeO_2 Nanoparticles and Their Oxygen Storage and Release Properties. *J. Phys. Chem. C* **2011**, *115*, 1740–1745.
39. Hojo, H.; Mizoguchi, T.; Ohta, H.; Findlay, S. D.; Shibata, N.; Yamamoto, T.; Ikuhara, Y. Atomic Structure of a CeO_2 Grain Boundary: The Role of Oxygen Vacancies. *Nano Lett.* **2010**, *10*, 4668–4672.
40. Haruta, M. Spiers Memorial Lecture Role of Perimeter Interfaces in Catalysis by Gold Nanoparticles. *Faraday Discuss.* **2011**, *152*, 11–32.
41. Guzman, J.; Carrettin, S.; Corma, A. Spectroscopic Evidence for the Supply of Reactive Oxygen during CO Oxidation Catalyzed by Gold Supported on Nanocrystalline CeO_2. *J. Am. Chem. Soc.* **2005**, *127*, 3286–3287.
42. Kim, H. Y.; Lee, H. M.; Henkelman, G. CO Oxidation Mechanism on CeO_2-Supported Au Nanoparticles. *J. Am. Chem. Soc.* **2012**, *134*, 1560–1570.
43. Shekhar, M.; Wang, J.; Lee, W.-S.; Williams, W. D.; Kim, S. M.; Stach, E. A.; Miller, J. T.; Delgass, W. N.; Ribeiro, F. H. Size and Support Effects for the Water−Gas Shift Catalysis over Gold Nanoparticles Supported on Model Al_2O_3 and TiO_2. *J. Am. Chem. Soc.* **2012**, *134*, 4700–4708.
44. Liu, Y; Tsunoyama, H; Akita, T; Tsukuda, T. Efficient and Selective Epoxidation of Styrene with TBHP Catalyzed by Au_{25} Clusters on Hydroxyapatite. *Chem. Commun.* **2010**, *46*, 550–552.
45. Gaur, S.; Miller, J. T.; Stellwagen, D.; Sanampudi, A.; Kumar, C. S. S. R.; Spivey, J. J. Synthesis, Characterization, and Testing of Supported Au Catalysts Prepared from Atomically-Tailored $Au_{38}(SC_{12}H_{25})_{24}$ Clusters. *Phys. Chem. Chem. Phys.* **2012**, *14*, 1627–1634.
46. Zhu, Y.; Qian, H.; Jin, R. Catalysis Opportunities of Atomically Precise Gold Nanoclusters. *J. Mater. Chem.* **2011**, *21*, 6793–6799.